LANGMUIR

pubs.acs.org/Langmuir Article

Diffusion of Solute Atoms in an Evaporated Liquid Droplet

Fuqian Yang,* Yong Li, and Kai Zhang

Cite This: *Langmuir* 2024, 40, 797−804 Read Online

ACCESS | Metrics & More | Article Recommendations

ABSTRACT: Controlling the evaporation of a solvent has made it possible to grow crystals, nanoparticles, and microparticles from liquid droplets. At the heart of this process is the evaporation-induced diffusion of solute atoms, causing the liquid solution of the solute atoms to be in a supersaturated state. In this work, we analyze the mass transport in a spherical liquid droplet, which experiences the loss or evaporation of the solvents across the droplet surface. Using a pseudo-steady-state method, two approximate solutions are derived for the moving boundary problem: one is a linear function of the square of radial variable with a constraint to the loss rate of the solvent, and the other is an exponential function of the square of radial variable without any constraint to the loss rate of the solvent. The numerical results obtained from both approximate solutions are in accord with the numerical results from the finite element method, validating the approximate solutions. The results reveal that a small evaporation/loss rate of the solvent is needed to maintain a relatively uniform distribution of solute atoms in a liquid droplet during the solvent evaporation/loss.

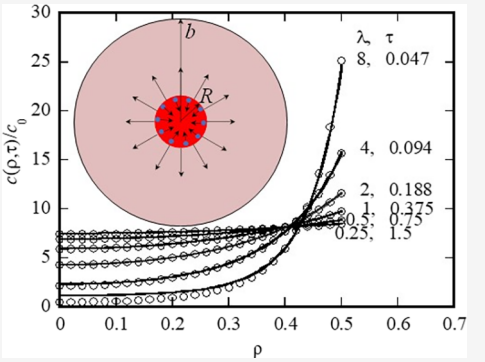

INTRODUCTION

Halide perovskites with unique properties of a large absorption coefficient,[1,2] tunable bandgap,[3,4] and high photoluminescence quantum yield[5,6] have attracted great interest in the applications of solar energy[7] and optoelectronics.[8] One of the challenges for the applications of halide perovskites is the structural degradation associated with the penetration of water molecules and light-induced phase segregation. This has stimulated research in the production of single-crystal films of halide perovskites.

There are generally three approaches available to produce single-crystal films of halide perovskites—bulk crystal slicing,[9,10] chemical vapor deposition,[11,12] and space-limited growth.[13−18] Among the three approaches, space-limited growth, which is based on the nucleation and growth of halide perovskite crystals in liquid solutions, has unique advantages of relatively high efficiency, tunable chemical compositions, limited loss of materials, and controllable film thickness. The nucleation and growth of halide perovskite crystals require the precursor solution to be supersaturated, which allows for the "deposition" and motion of monomers on the surfaces of the crystals to reach "equilibrium" positions. The continuous growth of single-crystal films of halide perovskites is dependent on the concentration of the precursor solution being maintained at a supersaturated state.

Currently, there are two approaches used in the space-limited growth of single-crystal films of halide perovskites. One involves isothermal loss/evaporation of the solvent in the precursor solution to maintain or increase the degree of supersaturation,[19] and the other is mainly based on the inverse-temperature principle of the decrease in solubility with increasing temperature.[20] Note that increasing temperature also causes the loss/evaporation of the solvent. The loss/evaporation of the solvent can be generally regarded as the diffusion of the solvent from the precursor solution to the surrounding environment across the free surface, which can lead to the redistribution of monomers in the precursor solution with the highest concentration of monomers at the free surface and likely hinder the growth of single-crystal films. There is a great need to understand the effects of the loss or evaporation of the solvent on the spatiotemporal evolution of the concentration of monomers in a liquid solution.

There are various mathematical models reported in literature[21−24] on the effects of the loss/evaporation of the solvent on the diffusion of solute atoms in an isolated liquid droplet and a sessile droplet, as reviewed by Erbil[25] and Sazhin et al.[26] Approximate solutions have been obtained under assumptions that the size of the droplet is maintained unchanged,[22] or the evaporation rate and the diffusion coefficient of solute atoms are constants.[21−24] Gardner[23] gave an asymptotic solution of the concentration of solute atoms in an evaporating drop with the conditions of constant evaporation rate and diffusion coefficient, and Gavin[24]

Received: October 5, 2023
Revised: December 1, 2023
Accepted: December 6, 2023
Published: December 19, 2023

presented an approximate solution of the problem. Currently, no analytical solutions are available, and numerical methods have been used to solve the related problems.[27−29] There has been great interest in obtaining analytical or approximate solutions of the problem, which can predict the spatiotemporal evolution of solute atoms in a liquid droplet in the synthesis of single-crystal films of halide perovskites and in the applications of particle engineering.

Realizing the importance in controlling the formation and growth of single-crystal films of halide perovskites and the need to have an analytical or approximate solution for the spatiotemporal evolution of the concentration of solute atoms in a liquid droplet during the solvent evaporation of the liquid droplet, we revisited the problem of the evaporation effects on the spatial distribution of solute atoms in a spherical liquid droplet. Following the method used by Langmuir,[21] we derived the evaporation/loss rate of the solvent across the surface of the liquid droplet. Approximate solutions of the spatiotemporal evolution of the concentration of solute atoms in the liquid droplet are obtained. Comparison between the approximate solutions and the numerical results from the finite element method is performed to validate the approximate solutions.

METHODS

Consider a spherical liquid droplet of radius R, which is enclosed in an air-filled spherical shell of the outmost radius b ($b \gg R$), as shown in Figure 1. The liquid droplet consists of the solvent and solute atoms

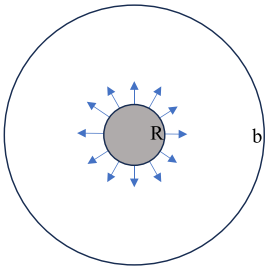

Figure 1. Schematic of a spherical liquid droplet of radius R enclosed in an air-filled spherical shell of the outmost radius b ($b \gg R$).

(or monomers). At the initial state ($t = 0$ with t as time), solute atoms (or monomers) are uniformly distributed in the droplet and the initial radius of the liquid droplet is R_0. The solvent in the liquid droplet experiences loss/evaporation at a rate of $\dot{m}_s$ (= dm_s/dt in the unit of moles per unit time) into the spherical shell. The loss/evaporation rates are the functions of temperature, chemical composition of the solvent, and size of the droplet. There are two diffusion zones—one is in the spherical shell for the diffusion of the solvent, and the other is in the droplet for the diffusion of the solute atoms (or monomers). For both diffusions, the corresponding diffusion coefficients are assumed to be constant. Note that the use of the spherical liquid droplet requires that the droplet size is smaller than the capillary length of $(\gamma/\rho g)^{1/2}$ (γ, surface tension; ρ, density; g, gravity). For a water droplet at room temperature, the capillary length is ∼2.7 mm. The spherical core−shell structure represents an ideal situation with the distance between adjacent droplets being much larger than the droplet size.

For the solvent diffusion in the spherical shell with $b \gg R$, the characteristic time is R^2/D_s (D_s as the diffusion coefficient of the solvent in the spherical shell); for the diffusion of solute atoms in the spherical droplet, the characteristic time is R^2/D (D is the diffusion coefficient of the solute atoms in the droplet). In general, there is $D_s \gg D$, yielding that the characteristic time of R^2/D_s is much smaller than the characteristic time of R^2/D. Thus, the diffusion of the solvent in the spherical shell can be approximated to be quasi-steady, as implicitly used by Langmuir.[21] The diffusion equation for the diffusion of the solvent in the spherical shell is

$$\frac{d^2c_s}{dr^2} + \frac{2}{r}\frac{dc_s}{dr} = 0 \tag{1}$$

with c_s as the concentration of the solvent in the unit of mole per unit volume. The boundary conditions are

$$c_s(b) = 0 \text{ and } c_s(R) = c_{s0} \tag{2}$$

Here, c_{s0} is the concentration of the solvent at the surface of the liquid droplet, which is assumed to be independent of the radius of the droplet. Note that the first equation in eq 2 can also be used for a constant concentration of the solvent, c_0, by introducing an auxiliary variable of $\tilde{c}\,(= c - c_0)$. The second equation is based on the condition that there is no convection present outside of the droplet. There likely exists the effect of the surrounding material, whose effect can be introduced by using the Gibbs−Thomson equation.[30]

The solution of eq 1 with the boundary conditions of eq 2 is

$$c_s = \frac{bRc_{s0}}{b - R}\left(\frac{1}{r} - \frac{1}{b}\right) \tag{3}$$

which gives the amount of the solvent per unit time (loss or evaporation rate), diffusing into the spherical shell as

$$\frac{dm_s}{dt} = -4\pi D_s R^2 \frac{\partial c_s}{\partial r}\bigg|_{r=R_0} = \frac{4\pi D_s bRc_{s0}}{b - R} \tag{4}$$

with m_s in the unit of mole. For $b \gg R$, eq 4 is simplified as

$$\frac{dm_s}{dt} = 4\pi D_s Rc_{s0} \tag{5}$$

which is the same as the result given by Langmuir.[21] According to the gas law,[31] there is $p = c_{s0}R_gT$ with p, R_g, and T as the pressure, gas constant, and absolute temperature, respectively. Substituting $p = c_{s0}R_gT$ in eq 5 yields the loss/evaporation rate of the solvent from the liquid droplet as

$$\frac{dm_s}{dt} = \frac{4\pi pD_s R}{R_gT} \tag{6}$$

The diffusion/evaporation of the solvent from the droplet into the spherical shell causes the shrinking of the droplet, and the volume change of the solvent can be calculated as

$$\frac{dV_s}{dt} = -\Omega_s\frac{dm_s}{dt} = -\frac{4\pi pD_s\Omega_s R}{R_gT} = -4\pi\alpha R \tag{7}$$

where V_s and Ω_s are the volume and molar volume of the solvent in the droplet, respectively. The parameter α is defined as

$$\alpha \equiv \frac{pD_s\Omega_s}{R_gT} \tag{8}$$

which has the same unit as the diffusion coefficient and can be regarded as the nominal diffusion coefficient of the solvent in the spherical shell.

For the diffusion of the solute atoms in the droplet, the diffusion equation is

$$\frac{\partial c}{\partial t} = D\left(\frac{\partial^2 c}{\partial r^2} + \frac{2}{r}\frac{\partial c}{\partial r}\right) \tag{9}$$

with c as the concentration of the solute atoms in the droplet in the unit of mole per unit volume. The volume of the droplet can be calculated as

$$V = \frac{4\pi}{3}R^3 \approx V_s + 4\pi\Omega_c\int_0^R cr^2 dr \tag{10}$$

https://doi.org/10.1021/acs.langmuir.3c02993
Langmuir 2024, 40, 797−804

where Ω_c is the molar volume of the solute atoms and r is the radial variable. Assuming that there is no change in the number/amount of the solute atoms during the diffusion/evaporation of the solvent into the spherical shell, we have

$$\frac{dV}{dt} = \frac{dV_s}{dt} \tag{11}$$

Substituting eqs 7 and 10 in eq 11 gives

$$\frac{dR}{dt} = -\frac{\alpha}{R} \tag{12}$$

whose solution is

$$R^2 = R_0^2 - 2\alpha t \tag{13}$$

with the condition of $R(0) = R_0$. It is evident that the size of the liquid droplet decreases with an increase in the diffusion/evaporation time, as expected.

The initial condition for the diffusion of the solute atoms in the droplet is

$$c(r, 0) = c_0 \tag{14}$$

and the boundary conditions are

$$\left.\frac{\partial c}{\partial r}\right|_{r=R} = -\frac{c}{D}\frac{dR}{dt} = \frac{\alpha}{D}\frac{c}{R} \text{ and } |c(0, t)| < \infty \tag{15}$$

The first equation in eq 15 is attributed to the shrinking of the liquid droplet, which causes the motion of the solute atoms at the surface of the droplet toward the droplet center.

We can follow the approach used by Schlünder[22] to introduce the dimensionless radius. This can reduce the above moving boundary problem to a fixed boundary problem with a modified partial differential equation for the diffusion of the solute atoms, which allows for the use of the separation of variables to solve the modified partial differential equation. See the Appendix section for the analysis. However, the operator of the derived "eigenequation" is not self-conjugated, and it is likely that no orthogonal eigenfunctions or eigenvalues can be obtained from the "eigenequation".

To solve the partial differential equation with the moving boundary and the initial boundary conditions, we use a pseudo-steady-state method[32,33] to approximately solve the problem. The steady-state solution of eq 9 is

$$c = A \tag{16}$$

which satisfies the second boundary condition in eq 15. Now, let the concentration of the solute atoms be

$$c(r, t) = A(t) + \frac{r^2 \dot{A}(t)}{6D} + \cdots \tag{17}$$

with $\dot{A}(t) = dA(t)/dt$. Substituting eq 17 with eq 15, one can easily show that eq 17 satisfies eq 15. Applying the boundary condition of eq 15 to eq 17 yields

$$\frac{R\dot{A}(t)}{3D} + \cdots = \frac{\alpha}{D}\frac{1}{R}\left(A(t) + \frac{R^2\dot{A}(t)}{6D} + \cdots\right) \tag{18}$$

To the order of $\dot{A}(t)$, eq 18 gives

$$\frac{R}{3D}\left(1 - \frac{\alpha}{2D}\right)\dot{A}(t) = \frac{\alpha}{D}\frac{A(t)}{R} \tag{19}$$

It needs to be pointed out that it requires $\dot{A}(t) > 0$, i.e., $\alpha < 2D$, to meet the condition of $\partial c/\partial r > 0$ at $r = R$. Substituting eq 13 in eq 19, we obtain the solution of $A(t)$ as

$$A(t) = A_0\left(1 - \frac{2\alpha t}{R_0^2}\right)^{-3/2(1-\alpha/2D)} \tag{20}$$

and the spatiotemporal evolution of the concentration of the solute atoms in the droplet to the order of $\dot{A}(t)$ as

$$c(r, t) = A_0\left(1 - \frac{2\alpha t}{R_0^2}\right)^{-3/2(1-\alpha/2D)} \left[1 + \frac{1}{2(1-\alpha/2D)}\frac{\alpha}{D}\frac{r^2}{R_0^2}\left(1 - \frac{2\alpha t}{R_0^2}\right)^{-1}\right] \tag{21}$$

with the parameter A_0 to be determined.

In general, it is expected that the parameter A_0 can be determined by the initial condition of eq 14. However, this can lead to the violation of the principle of mass conservation since there is no change in the solute atoms during the loss/evaporation of the solvent, as assumed. Thus, we determine the parameter A_0 from the mass conservation of the solute atoms, as given below

$$4\pi\int_0^R c(r, t)r^2 dr = \frac{4\pi}{3}R_0^3 c_0 \tag{22}$$

Equation 22 represents that the number of moles of the solute atoms remains unchanged during the loss/evaporation of the solvent. Substituting eq 21 in eq 22 yields

$$A_0 = c_0\left(1 - \frac{2\alpha t}{R_0^2}\right)^{-3/2+3/2(1-\alpha/2D)}\left[1 + \frac{3}{10(1-\alpha/2D)}\frac{\alpha}{D}\right]^{-1} \tag{23}$$

which gives the spatiotemporal evolution of the concentration of the solute atoms in the droplet as

$$\frac{c(r, t)}{c_0} = \left(1 - \frac{2\alpha t}{R_0^2}\right)^{-3/2}\left[1 + \frac{3}{10(1-\alpha/2D)}\frac{\alpha}{D}\right]^{-1} \left[1 + \frac{1}{2(1-\alpha/2D)}\frac{\alpha}{D}\frac{r^2}{R_0^2}\left(1 - \frac{2\alpha t}{R_0^2}\right)^{-1}\right] \tag{24}$$

It needs to be pointed out that the spatiotemporal evolution of the concentration of the solute atoms in the droplet given in eq 24 is only applicable with the condition of $\alpha < 2D$. Under the condition of $\alpha > 2D$, one likely needs to use numerical methods or other methods to obtain the spatiotemporal evolution of the concentration of the solute atoms in the droplet due to the loss or evaporation of the solvent in the droplet.

Realizing that eq 17 can be likely approximated as the Taylor series of an exponential function of r^2, we assume that the concentration of the solute atoms in the droplet can be expressed without constraint to the ratio of α/D as

$$c(r, t) = f(t)\exp\left(\frac{r^2}{6D}g(t)\right) \tag{25}$$

with $f(t)$ and $g(t)$ to be determined. Note that $f(t)$ and $g(t)$ in eq 25 are assumed to be independent. Using the boundary condition of eq 15, we obtain

$$g(t) = \frac{3\alpha}{R^2} \text{ and } c(r, t) = f(t)\exp\left(\frac{\alpha}{2D}\cdot\frac{r^2}{R^2}\right) \tag{26}$$

Substituting the second equation in eq 26 into eq 22 yields the function $f(t)$ as

$$f(t) = \frac{c_0}{3}\frac{\alpha}{D}\left(1 - \frac{2\alpha t}{R_0^2}\right)^{-3/2}\left(e^{\alpha/2D} - \sqrt{\frac{\pi D}{2\alpha}}\,\mathrm{erfi}\left[\sqrt{\frac{\alpha}{2D}}\right]\right)^{-1} \tag{27}$$

with $\mathrm{erfi}(z)$ as the imaginary error function $\mathrm{erf}(iz)/i$. Thus, the approximate solution of the spatiotemporal evolution of the concentration of the solute atoms in the droplet without constraint to the ratio of α/D is found to be

$$\frac{c(r, t)}{c_0} = \frac{1}{3}\frac{\alpha}{D}\left(1 - \frac{2\alpha t}{R_0^2}\right)^{-3/2}\left(e^{\alpha/2D} - \sqrt{\frac{\pi D}{2\alpha}}\,\mathrm{erfi}\left[\sqrt{\frac{\alpha}{2D}}\right]\right)^{-1} \exp\left(\frac{\alpha}{2D}\cdot\frac{r^2}{R^2}\right) \tag{28}$$

https://doi.org/10.1021/acs.langmuir.3c02993
Langmuir 2024, 40, 797−804

For the purpose of comparison, eq 25 is expanded in the Taylor series to the term r^2 as

$$c(r, t) = f(t)\left(1 + \frac{r^2}{6D}g(t) + O(r^4)\right) \tag{29}$$

Comparing eq 29 with eq 17 yields

$$f(t) = A(t) \text{and} f(t)g(t) = \dot{A}(t) \tag{30}$$

if it requires eq 25 that can be degenerated to eq 17 or the solution of eq 28 that can be degenerated to the solution of eq 24. However, $f(t)$ and $g(t)$ in eq 25 are treated as independent. Thus, the solution of eq 28 cannot be degenerated to the solution of eq 24.

RESULTS AND DISCUSSION

In the numerical calculation, we introduce the following dimensionless variables

$$\rho = r/R_0, \tau = Dt/R_0^2, \text{and } \lambda = \alpha/D \tag{31}$$

Using the dimensionless variables, eqs 24 and 28 can be written as

$$\frac{c(\rho, \tau)}{c_0} = (1 - 2\lambda\tau)^{-3/2}[1 + \frac{3\lambda}{10(1 - \lambda/2)}]^{-1} [1 + \frac{\lambda\rho^2}{2(1 - \lambda/2)(1 - 2\lambda\tau)}] \text{ for } \lambda < 2 \tag{32}$$

$$\frac{c(\rho, \tau)}{c_0} = \frac{\lambda}{3}(1 - 2\lambda\tau)^{-3/2}(e^{\lambda/2} - \sqrt{\frac{\pi}{2\lambda}}\,\text{erfi}[\sqrt{\frac{\lambda}{2}}])^{-1} \exp(\frac{\lambda\rho^2}{2(1 - 2\lambda\tau)}) \tag{33}$$

For comparison, the finite element method (FEM) was used to solve the moving boundary problem. Specifically, the partial differential equation with the moving boundary given in eq 13 was solved by using the PDE module of the commercial finite element package COMSOL Multiphysics. To ensure the convergence of numerical results, a one-dimensional finite element model with 1000 two-node linear elements was constructed in the radial direction of the spherical droplet, and the relative tolerance was set as 10^{-3}.

Figure 2 presents the spatial distribution of the concentration of solute atoms in a liquid droplet at different instances for λ = 0.25. The solid lines represent the FEM results; the cross symbols represent the results from eq 32, and the solid diamond symbols represent the results from eq 33. The FEM results and the results from eqs 32 and 33 exhibit similar trends. At the same instant, the concentration of the solute atoms decreases from the surface of the droplet toward the center of the droplet. At the same spatial position, the concentration of the solute atoms in the droplet increases with the increase in the evaporation time, as expected. Comparing the results from the numerical method, eqs 32 and 33, we note that there are no observable differences among these results for the dimensionless time larger than and equal to 0.2. This suggests that the approximations used in the pseudo-steady-state method and the exponential function with the boundary condition and the mass conservation likely are valid in solving the diffusion problem with the moving boundary condition. It needs to be pointed out that the results obtained from eqs 32 and 33 slightly deviate from the FEM results at a dimensionless time of 0.01 with the largest relative difference being less than 10%.

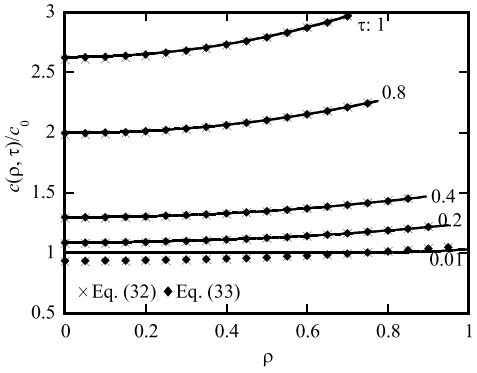

Figure 2. Spatial distribution of the concentration of solute atoms in a spherical liquid droplet at different instances for λ = 0.25. The solid lines represent the FEM results, the cross symbols represent the results from eq 32, and the solid diamond symbols represent the results from eq 33.

To further confirm the validity of eq 28 (eq 33) as an approximation of the solution of the concentration of solute atoms in an evaporated liquid droplet without any constraint to the ratio of α/D, we performed the FEM calculation of the spatial distribution of the concentration of solute atoms in a droplet for the ratios of α/D being 0.25, 0.5, 1, 2, 4, and 8 when the dimensionless radius of the droplet reaches 0.5. Figure 3 shows the numerical results of the spatial distribution of the concentration of the solute atoms in an evaporated liquid droplet. For comparison, the results obtained from eq 33 are also included in Figure 3, as represented by the open circle symbols. In general, the results obtained from eq 33 are in good accord with the FEM results. The largest deviation of the results obtained from eq 33 occurs at the center of the droplet with the ratio of α/D being 8. Both results reveal a rapid increase in the concentration of solute atoms at the surface of the droplet and the decrease in the concentration of solute atoms at the center of the droplet with increasing the ratio of α/D when the droplet reaches the same size under different ratios of α/D.

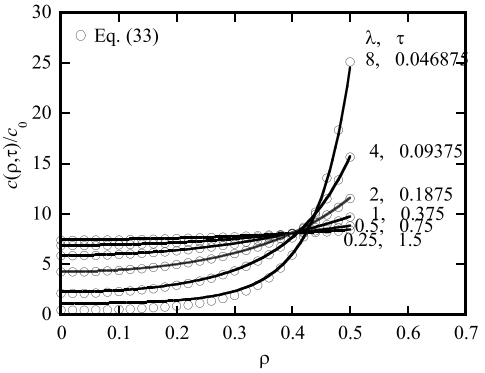

Figure 3. Spatial distribution of the concentration of solute atoms in an evaporated liquid droplet for ratios of α/D being 0.25, 0.5, 1, 2, 4, and 8 when the dimensionless radius of the droplet reaches 0.5. The solid lines represent the FEM results; the open circle symbols represent the results from eq 33.

Figure 4a,b shows the FEM results of the variations of the concentrations of solute atoms at the surface and center of an

https://doi.org/10.1021/acs.langmuir.3c02993
Langmuir 2024, 40, 797−804

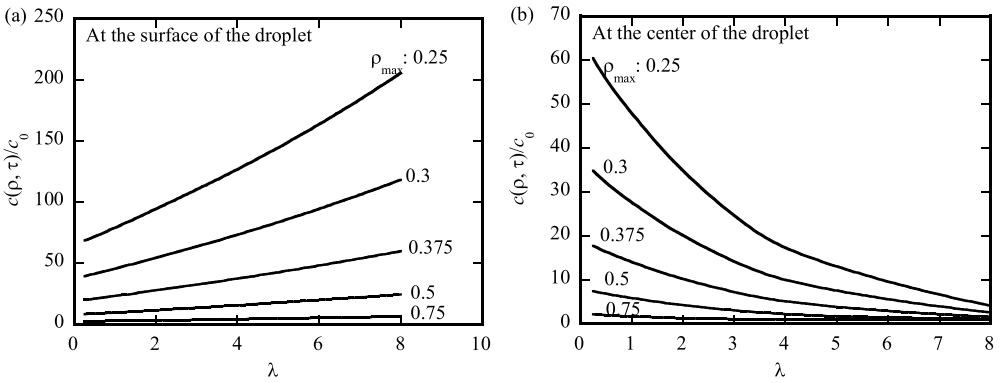

Figure 4. Variations of the concentrations of solute atoms in an evaporated liquid droplet with the ratio of α/D when the droplet reaches dimensionless sizes of 0.75, 0.5, 0.375, 0.3, and 0.25: (a) at the surface and (b) at the center.

evaporated liquid droplet with the ratio of α/D when the droplet reaches the same dimensionless sizes of 0.75, 0.5, 0.375, 0.3, and 0.25. It is evident that the larger the ratio of α/D, the higher the concentration of solute atoms at the surface of the droplet (Figure 4a) and the smaller the concentration of solute atoms at the center of the droplet (Figure 4b) for the evaporated droplet having the same dimensionless size. The ratio of α/D (the loss/evaporation rate) plays an important role in regulating the spatiotemporal evolution of the concentration of solute atoms in the droplet.

Note that the time for the evaporated droplet to reach the same dimensionless size is dependent on the numerical value of the ratio α/D, as shown in Figure 5. Increasing the ratio of

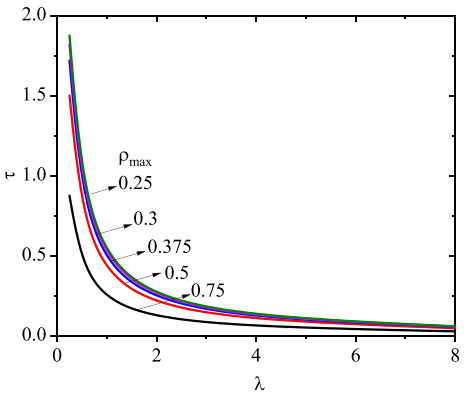

Figure 5. Variation of the dimensionless time with the ratio of α/D for the droplet to reach the same dimensionless sizes of 0.75, 0.5, 0.375, 0.3, and 0.25.

α/D reduces the time needed for the evaporated droplet to reach the same dimensionless size, as expected due to the "convection" effect on the motion of solute atoms near the surface of the droplet. This results in the increase in the concentration of solute atoms near the surface of the droplet and limits the increase in the concentration of solute atoms at the center of the droplet because of the requirement of mass conservation.

The asymptotic solution given by Gardner[23] has been widely used in particle engineering.[34−38] In the heart of the asymptotic solution given by Gardner[23] are the assumptions that the temporal evolution of the size of a spherical liquid droplet follows the first equation in eq 15, and the temporal evolution of the concentration of solute atoms in the droplet asymptotically follows the relation of $c \propto t^{3/2}$, in which Gardner analyzed the problem with a reversal time, i.e., the asymptotic solution was derived by considering the expansion of the droplet from a "zero-size" droplet. Gardner[23] obtained a differential equation independent of time and an asymptotic solution of the concentration of solute atoms in an exponential form. However, the spatial distributions of the concentration of solute atoms given by Gardner[23] at different instants are similar, and the ratio of the spatial distributions of the concentration of solute atoms at two different instants is only time-dependent. Such a result is different from those presented in Figure 2. Thus, the asymptotic solution given by Gardner[23] likely cannot represent the temporal evolution of the concentration of solute atoms in an evaporated droplet.

Recently, Sazhin et al.[26] proposed a model for the analysis of the drying of a liquid droplet, in which the analytical solution for the diffusion of species in the droplet was based on the condition of stationary boundary.[39] To address the problem of the moving boundary, they introduced an effective diffusivity with the proportionality coefficient being a function of the liquid Schmidt number and the Reynolds number of the liquid. Numerical calculations are required to determine the spatiotemporal distribution of the species. One challenging issue in applying the approach by Sazhin et al.[26,39] is the determination of the proportionality coefficient, which is likely dependent on the physical properties of the solvent and species, and it is unclear whether such a method can be applied to any liquid systems. On the other hand, the solution developed in this work is presented in a closed-form formulation, which can likely allow for the analysis of the spatiotemporal distribution of species in an evaporated droplet without multistep numerical calculations.

The analysis presented in this work is focused on an ideal situation in which a liquid droplet is isolated and suspended in space. In many cases, liquid droplets are present on the surface of solids or the effect of gravity is not negligible. Under such cases, the liquid droplets are in the form of a sessile or pendant shape. The problems are nonspherically symmetric. It would be very difficult, if not impossible, to obtain an approximate solution in a closed-form formulation. Numerical methods generally are needed to solve the problems.

Currently, the evaporation of the solvent in liquid droplets has been used to prepare micro- and nanoparticles, which involves nucleation and growth processes. According to thermodynamics, the onset of nucleation requires that the concentration of solute atoms (monomers) is larger than the solubility of the solute atoms (monomers), i.e., the liquid

https://doi.org/10.1021/acs.langmuir.3c02993
Langmuir 2024, 40, 797−804

solution is supersaturated. For a nonsupersaturated liquid droplet, the evaporation of the solvent can lead to an increase in the concentration of the solute atoms (monomers) and the evolution of the liquid solution to a supersaturated state. According to the results presented in Figure 3, the evaporation of the solvent can cause nonuniform distribution of the concentration of the solute atoms (monomers) and spatial distribution of the degree of supersaturation. The largest degree of supersaturation will be at the surface of the droplet, and nucleation starts to occur at the surface of the droplet. This trend makes it difficult to produce a single-crystal particle, monodisperse nanoparticles, or monodisperse microparticles for a large ratio of α/D, i.e., a large evaporation rate. To produce a single-crystal particle or monodisperse nanoparticles or microparticles, it generally requires that the concentration of solute atoms (monomers) in a droplet is relatively uniform. This indicates that a small ratio of α/D, i.e., a small evaporation rate, is needed to maintain a relatively uniform distribution of solute atoms during the evaporation of the solvent in a liquid droplet, as revealed in Figure 3.

CONCLUSIONS

In summary, we have analyzed the diffusion of solute atoms in a spherical liquid droplet, which experiences the loss of solvent through diffusion and evaporation across the droplet surface to the surrounding space. Under the condition that the transport of solvent atoms in the surrounding space can be described as a quasi-steady-state diffusion process, the shrinkage rate of the liquid droplet is found to be proportional to the diffusion coefficient of the solvent in the surrounding space and inversely proportional to the instant size of the liquid droplet. Using this relationship, the pseudo-steady-state method, and the principle of mass conservation, we have solved the moving boundary problem and obtained an approximate solution for the spatiotemporal evolution of the concentration of solute atoms in a spherical liquid droplet with a ratio of α/D less than 2. According to the approximate solution, we have proposed a general formulation for the spatiotemporal evolution of the concentration of solute atoms and obtained an approximate solution without any constraint to the ratio of α/D.

The comparison between the results obtained from the developed approximate solutions and the corresponding ones obtained from the FEM calculation has validated the approximate solutions and confirmed the applicability of the pseudo-steady-state method in analyzing the mass transport in an evaporated liquid droplet. The rapid increase in the concentration of solute atoms (monomers) at the surface of an evaporated liquid droplet with the evaporation time for a large ratio of α/D can lead to the nucleation and growth of nanoparticles near the droplet surface and polydisperse nanoparticles and/or microparticles. To produce nearly monodisperse nanoparticles or a single-crystal particle, a small ratio of α/D, i.e., a small evaporation rate, is needed to maintain a relatively uniform distribution of solute atoms in a liquid droplet during the evaporation of the solvent.

APPENDIX

Following the approach used by Schlünder,[22] we introduce a dimensionless variable of $\varsigma = r/R$, and eq 9 can be reformulated with the variable of ς as

$$\frac{\partial c}{\partial t} = \frac{D}{R^2}\left(\frac{\partial^2 c}{\partial \varsigma^2} + \frac{2}{\varsigma}\frac{\partial c}{\partial \varsigma}\right) + \frac{\varsigma}{R}\frac{\partial c}{\partial \varsigma}\frac{\mathrm{d}R}{\mathrm{d}t} \tag{A1}$$

Substituting eq 13 in eq A1 yields

$$\frac{\partial c}{\partial t} = \frac{D}{R^2}\left(\frac{\partial^2 c}{\partial \varsigma^2} + \frac{2}{\varsigma}\frac{\partial c}{\partial \varsigma}\right) - \frac{\alpha\varsigma}{R^2}\frac{\partial c}{\partial \varsigma} \tag{A2}$$

The initial conditions are

$$R(0) = R_0(0) \text{and } c(\varsigma, 0) = c_0 \tag{A3}$$

and the boundary conditions are

$$\left.\frac{\partial c}{\partial \varsigma}\right|_{\varsigma=1} = \frac{\alpha c}{D} \text{ and } |c(0, t)| < \infty \tag{A4}$$

in which the first equation indicates the migration of solute atoms toward the droplet center during the solvent evaporation.

Following the principle of the separation of variables, we introduce two auxiliary functions of $C(\varsigma)$ and $H(t)$ and express $c(\varsigma, t)$ as

$$c(\varsigma, t) = C(\varsigma)H(t) \tag{A5}$$

Substituting eq A5 in eq A2 yields

$$\frac{R^2}{D}\frac{1}{H}\frac{\mathrm{d}H}{\mathrm{d}t} = \frac{1}{C}\left(\frac{\mathrm{d}^2 C}{\mathrm{d}\varsigma^2} + \frac{2}{\rho}\frac{\mathrm{d}C}{\mathrm{d}\varsigma}\right) - \frac{\alpha\varsigma}{D}\frac{1}{C}\frac{\mathrm{d}C}{\mathrm{d}\varsigma} = \eta \tag{A6}$$

with η being a constant. For the function of $C(\varsigma)$, there is

$$\frac{\mathrm{d}^2 C}{\mathrm{d}\varsigma^2} + \left(\frac{2}{\varsigma} - \frac{\alpha\varsigma}{D}\right)\frac{\mathrm{d}C}{\mathrm{d}\varsigma} - \eta C = 0 \tag{A7}$$

Define $\lambda = \alpha/D$. The solution of eq A7 is found to be

$$C(\varsigma) = \frac{A}{\varsigma}\mathrm{H}\left[\frac{\lambda - \eta}{\lambda}, \frac{\sqrt{\lambda}\varsigma}{\sqrt{2}}\right] + \frac{B}{\varsigma}{}_1\mathrm{F}_1\left[-\frac{\lambda - \eta}{2\lambda}, \frac{1}{2}, \frac{\lambda\rho^2}{2}\right] \tag{A8}$$

where $\mathrm{H}[\bullet, \bullet]$ and ${}_1\mathrm{F}_1[\bullet, \bullet, \bullet]$ are the Hermite function and confluent hypergeometric function, respectively, and A and B are the two constants.

Substituting eq A8 in eq A4 yields

$$\frac{2^{1-\eta/a}\sqrt{\pi}A}{\Gamma\left[\frac{1}{2}\left(1 - \frac{a-\eta}{a}\right)\right]} + B = 0 \tag{A9}$$

$$\left(\frac{\sqrt{2}(a-\eta)}{\sqrt{a}}\mathrm{H}\left[-1 + \frac{a-\eta}{a}, \frac{\sqrt{a}}{\sqrt{2}}\right] - \mathrm{H}\left[\frac{a-\eta}{a}, \frac{\sqrt{a}}{\sqrt{2}}\right]\right) A - \left((a-\eta){}_1\mathrm{F}_1\left[1 - \frac{a-\eta}{2a}, \frac{3}{2}, \frac{a}{2}\right] + {}_1\mathrm{F}_1\left[-\frac{a-\eta}{2a}, \frac{1}{2}, \frac{a}{2}\right]\right)B = 0 \tag{A10}$$

To have non-zero solution, we obtain the following equation of η as

https://doi.org/10.1021/acs.langmuir.3c02993
Langmuir 2024, 40, 797−804

$$\left(\frac{\sqrt{2}(\lambda-\eta)}{\sqrt{\lambda}}\mathrm{H}\left[-1+\frac{\lambda-\eta}{\lambda},\frac{\sqrt{\lambda}}{\sqrt{2}}\right]-(1+\lambda)\right.$$
$$\left.\mathrm{H}\left[\frac{\lambda-\eta}{a},\frac{\sqrt{\lambda}}{\sqrt{2}}\right]\right)+\frac{2^{1-\eta/\lambda}\sqrt{\pi}}{\Gamma\left[\frac{1}{2}\left(1-\frac{\lambda-\eta}{\lambda}\right)\right]}$$
$$\cdot\left((\lambda-\eta)_1\mathrm{F}_1\left[1-\frac{\lambda-\eta}{2\lambda},\frac{3}{2},\frac{\lambda}{2}\right]+(1+\lambda)\right.$$
$$\left.{}_1\mathrm{F}_1\left[-\frac{\lambda-\eta}{2\lambda},\frac{1}{2},\frac{\lambda}{2}\right]\right)$$
$$=0 \tag{A11}$$

which determines the eigenvalues of η_n (n = 0, 1, 2, ...) if they exist. However, the operator for eq A11 is not self-conjugated, and it is likely that no orthogonal eigenfunctions and eigenvalues can be obtained from eq A11.

■ ASSOCIATED CONTENT

Data Availability Statement

The data that supports the findings of this study are available within the article.

■ AUTHOR INFORMATION

Corresponding Author

Fuqian Yang − *Materials Program, Department of Chemical and Materials Engineering, University of Kentucky, Lexington, Kentucky 40506, United States;* orcid.org/0000-0001-6277-3082; Email: fuqian.yang@uky.edu

Authors

Yong Li − *School of Intelligent Manufacturing and Control Engineering, Shanghai Polytechnic University, Shanghai 201209, China;* orcid.org/0000-0001-7607-0994

Kai Zhang − *School of Aerospace Engineering and Applied Mechanics, Tongji University, Shanghai 200092, China*

Complete contact information is available at: https://pubs.acs.org/10.1021/acs.langmuir.3c02993

Notes

The authors declare no competing financial interest.

■ ACKNOWLEDGMENTS

F.Y. is grateful for the support by the NSF through the grant CBET- 2018411 monitored by Dr. Nora F Savage.

■ REFERENCES

(1) He, X.; Deng, Y.; Ouyang, D.; Zhang, N.; Wang, J.; Murthy, A. A.; Spanopoulos, I.; Islam, S. M.; Tu, Q.; Xing, G.; Li, Y.; Dravid, V. P.; Zhai, T. Recent development of halide perovskite materials and devices for ionizing radiation detection. *Chem. Rev.* **2023**, *123*, 1207−1261.

(2) Song, W.; Qi, G.; Liu, B. Halide perovskite quantum dots for photocatalytic CO_2 reduction. *Journal of Materials Chemistry A* **2023**, *11*, 12482−12498.

(3) Lin, X.; Chen, L.; He, C.; Wang, Y.; Li, X.; Dang, W.; He, K.; Huangfu, Y.; Wu, D.; Zhao, B.; Li, B.; Li, J.; Duan, X. Vapor phase growth of centimeter-sized band gap engineered cesium lead halide perovskite single-crystal thin films with color-tunable stimulated emission. *Adv. Funct. Mater.* **2023**, *33*, No. 2210278.

(4) Nie, T.; Fang, Z.; Ren, X.; Duan, Y.; Liu, S. Recent advances in wide-bandgap organic−inorganic halide perovskite solar cells and tandem application. *Nano-Micro Lett.* **2023**, *15*, 70.

(5) Chen, Y.; Yin, J.; Wei, Q.; Wang, C.; Wang, X.; Ren, H.; Yu, S. F.; Bakr, O. M.; Mohammed, O. F.; Li, M. Multiple exciton generation in tin−lead halide perovskite nanocrystals for photocurrent quantum efficiency enhancement. *Nat. Photonics* **2022**, *16*, 485−490.

(6) Dutt, V. V.; Akhil, S.; Singh, R.; Palabathuni, M.; Mishra, N. Year-long stability and near-unity photoluminescence quantum yield of $CsPbBr_3$ perovskite nanocrystals by benzoic acid post-treatment. *J. Phys. Chem. C* **2022**, *126*, 9502−9508.

(7) Berhe, T. A.; Su, W.-N.; Chen, C.-H.; Pan, C.-J.; Cheng, J.-H.; Chen, H.-M.; Tsai, M.-C.; Chen, L.-Y.; Dubale, A. A.; Hwang, B.-J. Organometal halide perovskite solar cells: degradation and stability. *Energy Environ. Sci.* **2016**, *9*, 323−356.

(8) Du, P.; Wang, L.; Li, J.; Luo, J.; Ma, Y.; Tang, J.; Zhai, T. Thermal evaporation for halide perovskite optoelectronics: Fundamentals, progress, and outlook. *Adv.Opt. Mater.* **2022**, *10*, No. 2101770.

(9) Liu, Y.; Ren, X.; Zhang, J.; Yang, Z.; Yang, D.; Yu, F.; Sun, J.; Zhao, C.; Yao, Z.; Wang, B.; Wei, Q.; Xiao, F.; Fan, H.; Deng, H.; Deng, L.; Liu, S. F. 120 mm single-crystalline perovskite and wafers: towards viable applications. *Sci. China Chem.* **2017**, *60*, 1367−1376.

(10) Lv, Q.; Lian, Z.; He, W.; Sun, J.-L.; Li, Q.; Yan, Q. A universal top-down approach toward thickness-controllable perovskite single-crystalline thin films. *Journal of Materials Chemistry C* **2018**, *6*, 4464−4470.

(11) Chen, J.; Morrow, D. J.; Fu, Y.; Zheng, W.; Zhao, Y.; Dang, L.; Stolt, M. J.; Kohler, D. D.; Wang, X.; Czech, K. J.; Hautzinger, M. P.; Shen, S.; Guo, L.; Pan, A.; Wright, J. C.; Jin, S. Single-crystal thin films of cesium lead bromide perovskite epitaxially grown on metal oxide perovskite ($SrTiO_3$). *J. Am. Chem. Soc.* **2017**, *139*, 13525−13532.

(12) Wang, Y.; Shi, Y.; Xin, G.; Lian, J.; Shi, J. Two-dimensional van der Waals epitaxy kinetics in a three-dimensional perovskite halide. *Cryst. Growth Des.* **2015**, *15*, 4741−4749.

(13) Chen, Z.; Dong, Q.; Liu, Y.; Bao, C.; Fang, Y.; Lin, Y.; Tang, S.; Wang, Q.; Xiao, X.; Bai, Y.; Deng, Y.; Huang, J. Thin single crystal perovskite solar cells to harvest below-bandgap light absorption. *Nat. Commun.* **2017**, *8*, 1−7.

(14) Rao, H.-S.; Chen, B.-X.; Wang, X.-D.; Kuang, D.-B.; Su, C.-Y. A micron-scale laminar $MAPbBr_3$ single crystal for an efficient and stable perovskite solar cell. *Chem. Commun.* **2017**, *53*, 5163−5166.

(15) Yang, Z.; Deng, Y.; Zhang, X.; Wang, S.; Chen, H.; Yang, S.; Khurgin, J.; Fang, N. X.; Zhang, X.; Ma, R. High-performance single-crystalline perovskite thin-film photodetector. *Adv. Mater.* **2018**, *30*, No. 1704333.

(16) Deng, Y. H.; Yang, Z. Q.; Ma, R. M. Growth of centimeter-scale perovskite single-crystalline thin film via surface engineering. *Nano Convergence* **2020**, *7*, 1−7.

(17) Liu, Y.; Zhang, Y.; Yang, Z.; Yang, D.; Ren, X.; Pang, L.; Liu, S. Thinness- and shape-controlled growth for ultrathin single-crystalline perovskite wafers for mass production of superior photoelectronic devices. *Adv. Mater.* **2016**, *28*, 9204−9209.

(18) Di, H.; Jiang, W.; Sun, H.; Zhao, C.; Liao, F.; Zhao, Y. Effects of ITO substrate hydrophobicity on crystallization and properties of $MAPbBr_3$ single-crystal thin films. *ACS Omega* **2020**, *5*, 23111−23117.

(19) Chen, Y. X.; Ge, Q. Q.; Shi, Y.; Liu, J.; Xue, D. J.; Ma, J. Y.; Ding, J.; Yan, H. J.; Hu, J. S.; Wan, L. J. General space-confined on-substrate fabrication of thickness-adjustable hybrid perovskite single-crystalline thin films. *J. Am. Chem. Soc.* **2016**, *138*, 16196−16199.

(20) Tang, X.; Wang, Z.; Wu, D.; Wu, Z.; Ren, Z.; Li, R.; Liu, P.; Mei, G.; Sun, J.; Yu, J.; Zheng, F.; Choy, W. C. H.; Chen, R.; Sun, X. W.; Yang, F.; Wang, K. In situ growth mechanism for high-quality hybrid perovskite single-crystal thin films with high area to thickness ratio: looking for the sweet spot. *Adv. Sci.* **2022**, *9*, No. 2104788.

(21) Langmuir, I. The evaporation of small spheres. *Phys. Rev.* **1918**, *12*, 368−370.

(22) Schlünder, E. Temperatur-und massenänderung verdunstender tropfen aus reinen flüssigkeiten und wässrigen Salzlösungen. *Int. J. Heat Mass Transfer* **1964**, *7*, 49−73.

(23) Gardner, C. Asymptotic concentration distribution of an involatile solute in an evaporating drop. *Int. J. Heat Mass Transfer* **1965**, *8*, 667−668.
(24) Gavin, P. M. *A theoretical and experimental investigation of evaporation from drops containing nonvolatile solutes*. Ph D Disertation, University of Illinois at Urbana-Champaign: 1983.
(25) Erbil, H. Y. Evaporation of pure liquid sessile and spherical suspended drops: A review. *Adv. Colloid Interface Sci.* **2012**, *170*, 67−86.
(26) Sazhin, S. S.; Rybdylova, O.; Pannala, A. S.; Somavarapu, S.; Zaripov, S. K. A new model for a drying droplet. *Int. J. Heat Mass Transfer* **2018**, *122*, 451−458.
(27) Castillo, I.; Munz, R. J. Transient heat, mass and momentum transfer of an evaporating stationary droplet containing dissolved cerium nitrate in a rf thermal argon-oxygen plasma under reduced pressure. *Int. J. Heat Mass Transfer* **2007**, *50*, 240−256.
(28) Eslamian, M.; Ashgriz, N. Evaporation and evolution of suspended solution droplets at atmospheric and reduced pressures. *Drying Technology* **2007**, *25*, 999−1010.
(29) Widiyastuti, W.; Wang, W. N.; Lenggoro, I. W.; Iskandar, F.; Okuyama, K. Simulation and experimental study of spray pyrolysis of polydispersed droplets. *J. Mater. Res.* **2007**, *22*, 1888−1898.
(30) Gibbs, J. W. *The Collected Works of J. Willard Gibbs*. Longmans, Green and Co.: New York, 1928, *1*, 54−371.
(31) Lee, J. H.; Ramamurthi, K. *Fundamentals of Thermodynamics*. CRC Press: 2022; p 9−11.
(32) Bischoff, K. Accuracy of the pseudo steady state approximation for moving boundary diffusion problems. *Chem. Eng. Sci.* **1963**, *18*, 711−713.
(33) Liddell, K. C. Shrinking core models in hydrometallurgy: What students are not being told about the pseudo-steady approximation. *Hydrometallurgy* **2005**, *79*, 62−68.
(34) Vehring, R. Pharmaceutical particle engineering via spray drying. *Pharm. Res.* **2008**, *25*, 999−1022.
(35) Wei, Y.; Deng, W.; Chen, R.-H. Effects of insoluble nanoparticles on nanofluid droplet evaporation. *Int. J. Heat Mass Transfer* **2016**, *97*, 725−734.
(36) Malamatari, M.; Charisi, A.; Malamataris, S.; Kachrimanis, K.; Nikolakakis, I. Spray drying for the preparation of nanoparticle-based drug formulations as dry powders for inhalation. *Processes* **2020**, *8*, 788.
(37) Ahumada-Lazo, J. A.; Chen, R.-H. Effects of nanoparticle concentration and Peclet number on nanofluid droplet evaporation behavior. *International Journal of Thermal Sciences* **2022**, *178*, No. 107582.
(38) Boraey, M. A.; Vehring, R. Diffusion controlled formation of microparticles. *J. Aerosol Sci.* **2014**, *67*, 131−143.
(39) Sazhin, S. S.; Elwardany, A.; Krutitskii, P. A.; Castanet, G.; Lemoine, F.; Sazhina, E. M.; Heikal, M. R. A simplified model for bi-component droplet heating and evaporation. *Int. J. Heat Mass Transfer* **2010**, *53*, 4495−4505.

https://doi.org/10.1021/acs.langmuir.3c02993
Langmuir 2024, 40, 797−804